In vitro characterization, ADME analysis, and histological and toxicological evaluation of BM1, a macrocyclic amidinourea active against azole-resistant Candida strains

Francesco Orofino,[a] Giuseppina I. Truglio,[a] Diego Fiorucci,[a] Ilaria D'Agostino,[a] Matteo Borgini,[a] Federica Poggialini,[a] Claudio Zamperini,[b] Elena Dreassi,[a] Laura Maccari,[b] Riccardo Torelli,[c] Cecilia Martini,[d] Micaela Bernabei,[e] Jacques F. Meis,[f,g] Nitesh Kumar Khandelwal,[h] Rajendra Prasad,[i] Maurizio Sanguinetti,[c,d] Francesca Bugli[c,d,*], Maurizio Botta[a,b,j]

a Department of Biotechnology, Chemistry and Pharmacy, University of Siena, I-53100 Siena, 13 Italy
b Lead Discovery Siena s.r.l., Via Vittorio Alfieri 31, I-53019 Castelnuovo Berardenga, Italy
c Fondazione Policlinico Universitario "A. Gemelli" IRCCS, Dipartimento di Scienze di Laboratorio e Infettivologiche, Rome, Italy;
d Istituto di Microbiologia, Università Cattolica del Sacro Cuore, Rome, Italy
e Istituto di Anatomia Patologica, Università Cattolica del Sacro Cuore, Rome, Italy
f Department of Medical Microbiology and Infectious Diseases, Canisius-Wilhelmina Hospital, Nijmegen, The Netherlands
g Radboud University Medical Center, Nijmegen, the Netherlands
h School of Life Sciences, Jawaharlal Nehru University, New Delhi, 110067, India
I Amity Institute of Integrative Sciences and Health, Amity University, Gurgaon 122413, Haryana, India
j Sbarro Institute for Cancer Research and Molecular Medicine, Center for Biotechnology, College of Science and Technology, Temple University, BioLife Science Building, Philadelphia, PA 19122, USA.

Corresponding author
Email: Francesca.Bugli@unicatt.it,
Institute of Microbiology, Catholic University of Sacred Heart,
Largo F. Vito 1, 00168 ROME, ITALY,
Phone: +39-0630154964

TOC

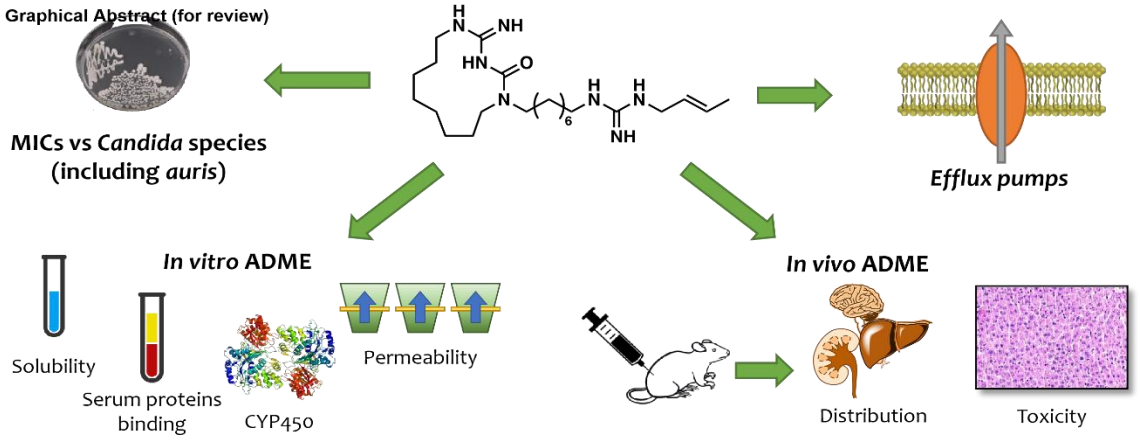

Highlights

- Macrocyclic amidinourea showed antifungal activity vs *Candida* spp., including *auris*
- *In vitro* and *in vivo* pharmacokinetics were evaluated
- *In vivo* toxicological and histological analyses were performed
- Data suggests the compound is suitable and safe for daily administration
- Valuable resource against renal and systemic infections

ABSTRACT

Background: Candida species are one of the most common causes of nosocomial bloodstream infections among the opportunistic fungi. Extensive use of antifungal agents, most of which were launched on the market more than 20 years ago, led to the selection of drug-resistant or even multidrug-resistant fungi. We recently described a novel class of antifungal macrocyclic compounds with an amidinourea moiety that is highly active against azole-resistant Candida strains. Objective: A compound from this family, BM1, was investigated in terms of in vitro activity against various Candida species, including C. auris isolates, interaction with the ABC transporter, CDR6, and in vivo distribution and safety. Methods: In vitro assays (CYP inhibition, microsomal stability, permeability, spot assays) were used to collect chemical and biological data; animal models (rat) paired with LC-MS analysis were utilised to evaluate in vivo toxicology, pharmacokinetics, and distribution. Results: The current research shows BM1 has a low in vivo toxicity profile, affinity for the renal system in rats, and good absorption, distribution, metabolism, and excretion (ADME). BM1 also has potent activity against azole-resistant fungal strains, including C. auris isolates and CDR6-overexpressing strains. Conclusions: The results confirmed low minimum inhibitory concentrations (MICs) against several Candida species, including preliminary data vs. C. auris. BM1 has good ADME and biochemical characteristics, is suitable and safe for daily administration and is particularly indicated for renal infections. These data indicate BM1 and its derivatives form a novel, promising antifungal class.

1. INTRODUCTION

Invasive fungal infections are life-threatening diseases that affect the bloodstream and other typically sterile body organs and are associated with long hospital stays and high costs for public health systems [1]. The pool of patients at risk increases every day and includes individuals undergoing major surgery or affected by AIDS or neoplasms [2,3]. Candida species account for most of the invasive infections among all the opportunistic fungi, causing 50% of nosocomial mycoses [4]. The increase in multidrug-resistant Candida strains, evolutionally selected by the use of antifungal agents introduced more than 25 years ago, worsens the situation [5-8]. Candida auris perfectly embodies this trend. This emerging multidrug-resistant pathogen gives rise to severe invasive fungal infections with high mortality, particularly among hospitalized patients. Echinocandins are the empirical drugs of choice vs. C. auris; however, not all isolates are susceptible, and resistance may develop during therapy. Therapeutic options for C. auris infections are limited; therefore, there is an urgent need for new, effective antifungal therapies [9]. We recently described a novel class of antifungal compounds that are highly active against various Candida strains [10-15]. These compounds comprise an amphiphilic macrocycle and a methylene linker ending with an alkenyl guanidine. A representative of this family, BM1 (Fig. 1), has recently been investigated in terms of its in vitro activity and in vivo safety, and has proven efficacy in treating immunocompetent mice systemically infected with both azolesusceptible and azole-resistant Candida strains [16]. Transcriptional analysis of the strains and fluorescence microscopy experiments confirmed the intracellular accumulation of the compound and revealed CDR1 and CDR2 (Candida drug resistance) genes overexpression [16]. CDRs encode for a series of promiscuous transporters

belonging to the ATP-binding cassette (ABC) family [17]. These transporters act as efflux pumps for many xenobiotics, including azole drugs such as fluconazole, pumping the drug out of the cytosol and preventing it from reaching its target. A recently described transporter, CDR6, has also been shown to impact on azole resistance [18]. Remarkably, BM1 has been shown to be highly active against strains overexpressing Cdr1 and Cdr2 efflux pumps. In the current study, the ADME profile, in vivo pharmacokinetics and acute toxicology of BM1 were thoroughly investigated after administration to rats, providing histological and toxicological analyses and focusing on renal distribution. The interaction between BM1 and the recently identified and characterized Candida ABC transporter, Cdr6 was also evaluated [18,19].

2. MATERIALS AND METHODS

2.1. BIOLOGICAL EVALUATION

2.1.1. Biological evaluation against *Candida* strains

The antimicrobial activity of BM1 was determined against 50 clinical isolates of Candida from 5 different species (albicans, tropicalis, glabrata, krusei, and parapsilosis) and 18 clinical isolates of C. auris. The latter were derived from patients with positive blood cultures in four hospitals in India, with known resistance profiles to fluconazole, voriconazole and echinocandins. Yeast cells were grown in yeast-peptone-dextrose (YPD) medium (Sigma-Aldrich, UK) for 16 h at 37°C and 150 rpm orbital shaker. Cells were then sub-inoculated in fresh YPD medium and grown to an optical density (OD) of 0.3. The turbidity of the inoculum was adjusted to 0.5 McFarland and diluted 1:500 in RPMI 1640 broth, corresponding to around 2.5 × 105 CFU/mL. Minimal inhibitory concentrations (MICs) were determined by liquid growth inhibition assays by standard procedures using serial dilutions of BM1 dissolved in an appropriate buffer with a final concentration from 256 to 0.125 µg/mL in a 96-well flat-bottom Microtiter® plate [20]. Plates were incubated at 35°C, and MIC values were visualized after 24 h as the lowest concentration of BM1 that completely inhibited cell growth

2.1.2. Heterologous overexpression of CDR6 in S. cerevisiae strain

A heterologous CDR6-overexpressing C. albicans strain was constructed by PCR amplification of the CDR6 gene from genomic DNA of C. albicans SC5314 using CDR6-PacI-FP and CDR6-NotI-RP primers (Supplementary Table ST4) and cloned into the pABC3- GFP vector at the PacI and NotI restriction site. This CDR6 genecontaining plasmid (pABC3-CDR6-GFP) was digested with AscI and the transformation cassette was used to transform S. cerevisiae AD(1-8)u− cells using the lithium acetate method to produce strain AD-CDR6 [21,22]. The susceptibility of these strains was evaluated by spot dilution assay as described previously [19]. Briefly, a 5- fold serial dilution of 0.1 OD600 culture in 0.9% saline was prepared from overnight cultures and 5 µL from each dilution were spotted on to Yeast Extract-Peptone-Dextrose (YEPD) agar plates containing berberine (BER, 75 or 100 µg/mL), rhodamine 123 (R123, 4 µg/mL), fluconazole (FLC, 16 µg/mL), or test compound (BM1, 4.65 µg/mL) and the plates were incubated at 30°C for 48 h. The expression levels of CDR6 gene in C. albicans clinical isolates (Gu4 and Gu5) were measured by semiquantitative RT-PCR and ACT1 gene was used as an expression control as described previously [19]. The details of the method are provided in the supplementary data.

2.2. *IN VITRO* ADME

2.2.1. Solubility Assay

Solid BM1 (1.0 mg) was added to 1.0 mL of distilled water. The sample was shaken in a shaker bath at room temperature for 24 h. The suspension was filtered through a 0.45-µm nylon filter (Acrodisc) and the solubilized compound was quantified in triplicate using the chromatographic method 1, reported in the supplementary data.

2.2.2. Binding Fluorimetric Assay

The binding of BM1 to human serum albumin (HSA) and α-1-acid glycoprotein (AGP) was monitored by fluorescence spectroscopy to determine the dissociation constant (Kd). Results were validated using warfarin and chlorpromazine (characterized by high affinity for HSA and AGP, respectively) as standard ligands and by referring to previously reported data [23-25]. A quantitative analysis of the potential interaction was performed by fluorimetric analysis using 96 multiwell plates: in each well a defined concentration of HSA or AGP (10 µM in phosphate buffer 1 mM) was added with different amounts of tested compound (0.1 µM to 500 µM from stock solutions in dimethylsulfoxide [DMSO]). Plates were gently shaken for 30 min at room temperature for equilibration. Spectra were recorded from 300 to 400 nm after excitation at 295 nm using a Perkin Elmer EnVision Multilabel Reader 2014 spectrofluorimeter equipped with EnVision Manager ver.1.13 software. Kd values were calculated using GraphPad software (version 6.0) using nonlinear square regression and two phase decay functions.

2.2.3. Parallel Artificial Membrane Permeability Assay (PAMPA)

A phosphate buffer (pH 7.4, 0.025 M) solution of BM1 0.5 mM was prepared (donor solution). The filters present in the donor plate were coated with 5 µL of a 1% (w/v) dodecane solution of phosphatidylcholine. Donor solution (150 µL) was added to each well of the filter plate; 300 µL of phosphate buffer solution were added instead to each well of the acceptor plate. BM1 was tested in two different plates on different days. The sandwich was incubated for 5 h at room temperature with gentle shaking. Plates were separated and samples were taken from both receiver and donor sides. In these samples, BM1 was quantified using the chromatographic method 1, reported in the supplementary data. Papp value was calculated as reported in the supplementary data.

2.2.4. Microsomal Stability Assay

A DMSO solution of BM1 was incubated at 37°C for 60 min in 125 mM phosphate buffer (pH 7.4) and 5 µL of human liver microsomal protein (0.2 mg/mL), in the presence of an NADPHgenerating system at a final volume of 0.5 mL (50 µM final compound concentration); DMSO did not exceed 2% (final solution). The reaction was stopped by cooling in ice and adding 1.0 mL of acetonitrile. The reaction mixtures were centrifuged, and the parent drug and metabolites determined by LC-UV-MS using the chromatographic method 2, reported in the supplementary data. The percentage of non-metabolized compound was calculated by comparison with reference solutions.

2.2.5. CYP450 inhibition study

The inhibition of cytochrome P450 3A4 isoform by BM1 was measured by determining its conversion of the substrate testosterone to 6β-hydroxytestosterone (CYP3A4-specific reaction) [26], a much-reported methodology and an ideal standard [27-30]. The amount of 6β-hydroxylated metabolite was measured in the presence and absence of BM1 and ketoconazole (testosterone concentration of 100 µM in phosphate buffer 0.025 M, pH 7.4), a standard selective inhibitor of CYP3A4 [31,32]. Compounds were solubilized in DMSO and added in a test-tube to give final concentrations of 1, 10, 25, 50 and 0.01, 0.05, 0.5, 5 µM, for BM1 and ketoconazole, respectively. Incubations were performed in a mixture containing human liver microsomes (1.0 mg/mL of protein) in phosphate buffer 0.025 M, pH 7.4 and NADPH (200 µM) previously solubilized in an MgCl2 48 mM solution. The final incubation volume was 0.25 mL. After a 40-min incubation at 37°C, the reaction was stopped by adding 1.0 mL of acetonitrile in the presence of corticosterone 2 µM as internal standard. Samples were centrifuged for 20 min at 5000 rpm. Concentrations of testosterone and its metabolite, 6βhydroxytestosterone were determined using the chromatographic method 2, reported in the supplementary data.

2.3. IN VIVO ADME

2.3.1. *In vivo* pharmacokinetics and renal tract distribution

For the in vivo pharmacokinetic assay, 3 groups of 3 healthy male rats received a different single dose of BM1, 2 and 10 mg/kg through intravenous (IV) injection and 20 mg/kg per os (PO). For the IV administration, water plus 10% v/v N-methyl-2-pyrrolidone and kolliphore EL 20% w/v was used, whereas for PO, 0.5% Tween 80 was added to the same vehicle. Blood samples were collected from the tail vein at various time points (5', 15', 30', 1 h, 2 h, 4 h, 6 h, and 24 h). After 24 h, rats were sacrificed and brain, liver and kidneys samples were collected and analysed to measure the residual amount of compound. For the renal tract distribution, a first group of 3 rats received the dose of 2.0 mg/kg each. A second control group of 3 rats was treated with vehicle only. Rats were all injected by IV administration via the tail vein, once daily for 6 days. Observations were made twice daily for clinical signs of pharmacological and toxicological effects of the treatment and urine samples were collected for the first 3 days and the last day, by placing the animals in the metabolic chamber. Tissues samples (kidney, bladder, liver, and brain) were collected at day 6. Blood samples were centrifuged at 5000 rpm for 20 min to separate the plasma fraction, which was collected in a test tube. Acetonitrile (with internal standard at the concentration of 0.3 µg/mL) was added to each sample to denature proteins. Samples were centrifuged at 5000 rpm for 20 min, and the supernatant was recovered, dried under vacuum and solubilized again in methanol (100 µL). Organs were homogenized using a T10 basic ULTRA-TURRAXR homogenizer (Bioclass, Pistoia, Italy); acetonitrile internal standard solution was added to extract the compound from the tissue, and the homogenate was centrifuged at 5000 rpm for 20 min. The supernatant was recovered and filtered. Urine samples were processed similarly to plasma fractions. BM1 was quantified in the processed samples using the chromatographic method 1, reported in the supplementary data. The matrix effect was also evaluated.

2.3.2. *In vivo* toxicology

The experimental design includes 3 treatment groups of 6 male adult rats and 1 additional control group of 3 rats. Treatment groups were administered with a different single-dose concentration of BM1 and the control group was inoculated with vehicle only. Animals were weighed individually on day 1 and after 3 days at sacrifice. The compound was injected via the tail vein in a single systemic dose (0.2 mL/dose) at dose levels of 0.5, 2 and 10 mg/kg of body weight. Observations were made twice daily for clinical signs of pharmacological and toxicological effects of the treatment. 24, 48 and 72 h post-inoculum, 2 rats from each treatment group and 1 rat from the vehicle group were sacrificed and liver, kidneys, heart, spleen, and brain samples were collected for histopathological examination. Sections of 2 µm thickness were taken using a microtome, processed in alcohol-xylene series, and stained with haematoxylin and eosin. Histopathological changes in tissue specimens were assessed in at least 5 randomly selected tissue sections from each organ for all rats of the groups under study.

3. RESULTS AND DISCUSSION

3.1. BIOLOGICAL EVALUATION

3.1.1. *In vitro* antimicrobial activities against *Candida* spp. Isolates

Antimicrobial activities of BM1 against various Candida spp. are summarized in Table 1. Details of single strain MICs and activities of different classes of conventional antifungals against C. auris isolates are reported in detail in Supplementary Tables ST1 and ST2. Susceptibility breakpoints for C. auris have not yet been defined by either the Clinical and Laboratory Standards Institute (CLSI) or the European Committee on Antimicrobial Susceptibility Testing (EUCAST). Hence, the information given above should be considered as indicative and not as breakpoints that define resistance. Although these are still preliminary data, it was intriguing to find that the C. auris strain for which MICs of fluconazole were the lowest (Strain 1a, Supplementary Table ST2) is

the one on which BM1 presented the highest MIC (64 µg/mL), while other strains more susceptible to BM1 (with MICs ranging from 8 to 32 µg/mL) are those with the highest azole antifungal resistance profiles. Notably, BM1 presented an MIC of 16 µg/mL against echinocandin-resistant strains (e.g. strain 45, Supplementary Table ST2). Phylogenetically, C. auris is related to and can be confused with Candida haemulonii [33], which is known for its intrinsic resistance to fluconazole and amphotericin B. Genetic and molecular mechanisms of azoles resistance of C. auris have yet to be clarified in detail. An in vivo study using a murine model of invasive candidiasis is necessary to compare the treatment effects of BM1 with those of conventional antifungals.

Also, BM1 showed good to excellent MICs against more common species. The most sensitive was C. albicans (with MICs as low as 0.125 µg/mL), followed by C. tropicalis and C. parapsilosis, whereas C. glabrata and C. krusei were the less sensitive pathogens, except for a few strains. 3.1.2. Importance of the ABC

3.1.2. Importance of the ABC transporter *CDR6* for the activity of 1

Our previous microarray data in the presence of BM1 showed that three ABC transporters (CDR1, CDR2, and CDR6/orf19.4531) were significantly up-regulated in C. albicans and we successfully proved how important was the presence of CDR1 and CDR2 transporters in C. albicans for the susceptibility to BM1 [16]. Recently, a new member of the ABC superfamily was identified and characterized (CDR6/orf19.4531); this is localized into the plasma membrane similar to CDR1 and CDR2 [19,34]. To test whether CDR6 also impacts on the susceptibility towards BM1 in C. albicans similar to CDR1 and CDR2, spot analysis of C. albicans WT (SC5314) and CDR6 null mutant (cdr6—/—) strains was performed in the presence of BM1. Surprisingly, there was no detectable change in susceptibility towards BM1 (data not shown). This could be caused by the presence of CDR1 and CDR2 transporters in cdr6—/— mutant, which could compensate for the impact of the absence of CDR6. To overcome this issue and to test the sole impact of CDR6 on BM1 activity, we exploited the heterologous overexpression system of S. cerevisiae AD(1-8)u− strain, which is frequently used for expression and functional characterization of the transporters from Candida and other similar yeasts [22,35]. This S. cerevisiae AD1-8u− strain lacks 7 ABC transporters (ScYor1p, ScPdr5p, ScPdr10p, ScSnq2p, ScPdr11p, ScPdr15p, and ScYcf1p), thus providing a cleaner background by ensuring minimum masking effects due to major ABC transporters of the host. Thus, the C. albicans Cdr6 transporter was overexpressed in S. cerevisiae AD(1-8)u− strain and the resulting derivatized strain was designated as AD-CDR6. Spot assays were performed on AD-CDR6 and its parental strain AD(1-8)u− in YEPD agar plates in the presence of berberine (BER), rhodamine 123 (R123) and BM1. The AD-CDR6 strain displayed resistance towards BER and R123 compared with its parental AD(1-8)u− strain (Fig. 2). This confirmed the functional overexpression of the Cdr6 transporter in the AD-CDR6 strain as berberine (BER) and rhodamine 123 (R123) are known substrates of Cdr6 [19]. Interestingly, AD-CDR6 showed a higher susceptibility to BM1 compared with the parental AD(1-8)u− strain, indicating that, as with Cdr1 and Cdr2, the presence of the Cdr6 transporter makes the cell susceptible towards BM1. The impact of these ABC transporters was further confirmed in clinical isolate match pairs of C. albicans, where CDR1, CDR2, and CDR6 were simultaneously overexpressed in azole-resistant isolate Gu5 compared with sensitive isolate Gu4 [36] (Fig. 3a). As can be seen in Fig. 3b, clinical isolates overexpressing CDR6, CDR2, and CDR1 showed resistance towards fluconazole but were highly susceptible to the presence of BM1. This finding confirms previous observations: there is a positive correlation between the presence of ABC transporters and the order of activity of BM1. The transporters are involved in the mode of action of this compound in a way we still do not completely understand. They could be involved in the uptake process, thus their presence would enhance the activity of BM1 by increasing the amount of compound in the cellular compartment. Although there is no definitive proof of this supposition, the current data clearly indicate that overexpression of the ABC

transporters is associated with a phenotype favouring the entry, but not the efflux, of the compound and consequently renders azole-resistant fungal strains more susceptible to the fungicidal action of BM1.

3.2. *IN VITRO* ADME RESULTS

3.2.1. Water solubility, binding to serum proteins, permeability assay

Compound **1** presented a good water solubility and a one-site binding kinetics for plasmatic proteins HSA and AGP (Table 2), with higher affinity for AGP than HAS (20-fold lower affinity for the latter). These results could be expected since AGP has the ability to bind cationic molecules with higher efficiency.[37]

Passive permeability was evaluated by PAMPA, which simulated the composition of the lipidic intestinal lumen. It presented a low passive permeability, which is counterbalanced by its good water solubility during the distribution process. All the data are reported in Table 2.

3.2.2. Microsomal Stability Assay and CYP450 inhibition

The susceptibility of BM1 to metabolism in the presence of human liver microsomal protein was evaluated to understand if its metabolism could involve CYP-oxidative pathways. BM1 exhibited high metabolic stability: 95% of the unmodified parent compound was detected (Table 2) and no potentially inactive oxidized derivatives were detected. The inhibition of BM1 towards CYP3A4 was determined as this isoform is involved in the first line of xenobiotic processing, in the occurrence of several drug-drug interactions, drug toxicity, reduced pharmacological effect, and adverse drug reactions [38,39]. The amount of 6β-hydroxytestosterone in the control mix and in the samples with added BM1 was not significantly different ($P > 0.05$). These data indicate that BM1 does not inhibit CYP3A4 activity (Fig. 4, panel A). As azole antifungals are known CYP450 inhibitors this information is important in terms of potential coadministration [39]. This could pave the way to a synergic effect evaluation. Data for ketoconazole, used to validate our method, are also reported (Fig. 4, panel B).

3.3. *IN VIVO* ADME RESULTS

3.3.1. *In vivo* pharmacokinetics

The in vivo pharmacokinetic experiment was conducted using rats to obtain insights about BM1 distribution. Both IV injection and PO administration were considered. The levels of BM1 in plasma following PO administration were lower than the limit of quantification. On the other hand, trend of plasma levels at 2 and 10 mg/kg IV, expressed as µg of BM1 per mL of plasma vs. time, was quantifiable and can be seen in Fig. 5. The results indicated a first-order kinetic; pharmacokinetics parameters were calculated and reported in Table 3. Oral bioavailability of BM1 could be further tested using higher doses in the future. The low oral bioavailability of the compound could be linked to its low permeability (as shown from PAMPA). This common problem in drug development could be overcome by adjusting the drug formulation, e.g. by incorporating permeability enhancers or increasing local luminal concentration. The first-order kinetic after IV administration indicates a constant fraction of the drug is eliminated during the treatment. As supported by the pharmacokinetic values reported in Table 3, such as the Cmax and AUC t1/2, this clearly shows that BM1 is compatible with daily administrations. Analyses of tissue samples from brain, liver, and kidneys are shown in Fig. 6. Brain levels were close to the detection limit, so were considered null; therefore, BM1 is not suitable to cross the blood-brain barrier. No noteworthy accumulation was observed in liver tissue. There was a significant concentration of BM1 in renal tissue, as may be expected given the good hydrophilicity of the compound, which routes BM1 to renal excretion. These data, along with its metabolic stability, indicate that BM1 did not tend to accumulate in a particular organ or tissue and that renal excretion could be the only significant elimination route.

3.3.2. Renal and urinary tract distribution

To further investigate the affinity of BM1 to kidneys shown in previous pharmacokinetic analyses, an additional study was performed that specifically focused on the urinary tract to identify potential target organs of BM1. Tissue and urine analyses data are summarized in Fig. 7.

During treatment, tails of all animals, including those in the control group, did not present any suffering or inflammation. No animal died before the endpoint. Again, brain levels were lower than the limit of detection, and bladder levels were comparable to that of the liver. Kidneys showed greater concentrations of unmodified compound, which were also detected in urine samples. These results are compatible with BM1 being rapidly filtered through the glomerular capillaries, then entering the nephron and being reabsorbed, thus concentrating in the tubular lumen from which it is then slowly and regularly excreted through urine. The results of the urine analysis confirm the hypothesis of renal elimination of BM1 in concentrations of 2-3 µg/mL, while it is able to reach higher concentrations (up to 25.7 µg/g) in kidneys. These values are comparable or higher than MICs for many Candida strains; therefore, BM1 is a valuable option for the treatment of urogenital infections.

3.3.3. *In vivo* toxicology

In vivo experiments were performed to exclude tissue damage or acute toxicity events. Representative images of the histological examination sections, stained with haematoxylin and eosin, of brains, livers, spleens, and kidneys from rats are provided in the supplementary material (Supplementary Figure 2 and 3). There were no clinical signs of toxicological effects during the daily observations of living animals and no obvious alterations in cellular morphology of organs from treated vs. untreated rats from the histological analysis. Animal behaviour and wellness were not compromised during the treatment period. These data strongly support the safety of BM1 in clinical use.

4. CONCLUSION

In this work, we investigated a representative of a novel class of antifungal compounds. The ADME profile of BM1 is excellent, with good solubility and microsome stability, and it does not inhibit human cytochrome activity; but, as a downside, it has low passive permeability, which could be expected given its good hydrophilicity. We verified the activity of BM1 against azole-resistant fungal strains, overexpressing efflux pumps, which is a key feature in novel promising drugs. Early data on its activity against C. auris strains have been collected and the results are encouraging. This compound could be a valuable treatment option to defeat fungal systemic infections in the future, and, currently it appears to be a valid option for the treatment of renal infections, where it accumulates to concentrations higher than most of the MICs it showed for Candida species, such as albicans, tropicalis and parapsilosis.

ACKNOWLEDGMENT

The authors thank Professor Anuradha Chowdhary, Vallabhbhai Patel Chest Institute, University of Delhi (Delhi, India), for kindly providing *C. auris* strains.

DECLARATIONS

Funding.

Authors acknowledge funding from ICMR (AMR/149/2018-ECD-II) and DBT (BT/PR14117/BRB/10/1420/2015) and for Senior Research Fellowship from University Grant Commission. Financial support by the Italian Ministry of University and Research (Linea D1 Università Cattolica del Sacro Cuore, FB) is also gratefully acknowledged. This work was partially funded by Cygnet Biosciences B.V., Kaya Richard J. Beaujon Z/N, Curaçao.

Competing Interests: None

Ethical Approval.

Animal studies were conducted under a protocol approved by the Institutional Animal Use and Care Committee at Università Cattolica del Sacro Cuore, Fondazione Policlinico Universitario Agostino Gemelli IRCCS (permit no. 21.05) and authorized by the Italian Ministry of Health (Protocol number: 1F295.13, 2/05/2016; Authorization number: 707/2016-PR, 22/08/2016) according to the Legislative Decree 116/92, which implemented the European Directive 86/609/EEC on laboratory animal protection in Italy.

REFERENCES

[1] Morgan J, Meltzer MI, Plikaytis BD, Sofair AN, Huie-White S, Wilcox S, et al. Excess mortality, hospital stay, and cost due to Candidemia: a case-control study using data from population-based candidemia surveillance. Infect Control Hosp Epidemiol 2016;26:540–7. doi:10.1086/502581.

[2] Höfs S, Mogavero S, Hube B. Interaction of Candida albicans with host cells: virulence factors, host defense, escape strategies, and the microbiota. J Microbiol 2016;54:149–69. doi:10.1007/s12275-016-5514-0.

[3] Pappas PG. Invasive candidiasis. Infect Dis Clin North Am 2006;20:485–506. doi:10.1016/j.idc.2006.07.004.

[4] Fernández-García R, de Pablo E, Ballesteros MP, Serrano DR. Unmet clinical needs in the treatment of systemic fungal infections: The role of amphotericin B and drug targeting. Int J Pharm 2017;525:139–48. doi:10.1016/j.ijpharm.2017. 04.013.

[5] Anderson JB. Evolution of antifungal-drug resistance: mechanisms and pathogen fitness. Nat Rev Micro 2005;3:547–56. doi:10.1038/nrmicro1179.

[6] Arendrup MC, Patterson TF. Multidrug-resistant Candida: epidemiology, molecular mechanisms, and treatment. J Infect Dis 2017;216:S445–51. doi:10.1093/ infdis/jix131.

[7] Srinivasan A, Lopez-Ribot JL, Ramasubramanian AK. Overcoming antifungal resistance. Drug Discov Today Technol 2014;11:65–71. doi:10.1016/j.ddtec.2014. 02.005.

[8] Wiederhold N. Antifungal resistance: current trends and future strategies to combat. Infect Drug Resist 2017;10:249–59. doi:10.2147/IDR.S124918.

[9] Tsay S, Kallen A, Jackson BR, Chiller TM, Vallabhaneni S. Approach to the investigation and management of patients with Candida auris, an emerging multidrug-resistant yeast. Clin Infect Dis 2018;66:306–11. doi:10.1093/cid/ cix744.

[10] Manetti F, Castagnolo D, Raffi F, Zizzari AT, Rajamaki S, D'Arezzo S, et al. Synthesis of new linear guanidines and macrocyclic amidinourea derivatives endowed with high antifungal activity against Candida spp. and Aspergillus spp. J Med Chem 2009;52:7376–9. doi:10.1021/jm900760k.

[11] Dreassi E, Zizzari AT, D'Arezzo S, Visca P, Botta M. Analysis of guazatine mixture by LC and LC-MS and antimycotic activity determination of principal components. J Pharm Biomed Anal 2007;43:1499–506. doi:10.1016/j.jpba.2006.10. 029.

[12] Sanguinetti M, Sanfilippo S, Castagnolo D, Sanglard D, Posteraro B, Donzellini G, et al. Novel macrocyclic amidinoureas: potent non-azole antifungals active against wild-type and resistant Candida Species. ACS Med Chem Lett 2013;4:852–7. doi:10.1021/ml400187w.

[13] Maccari G, Deodato D, Fiorucci D, Orofino F, Truglio GI, Pasero C, et al. Design and synthesis of a novel inhibitor of T. viride chitinase through an in silico target fishing protocol. Bioorg Med Chem Lett 2017;27:3332–6. doi:10.1016/j. bmcl.2017.06.016.

[14] Borgini M, Orofino F, Truglio GI, Balestri L, Botta M. A gram-scale synthesis of a macrocyclic amidinourea with strong antifungal activity through a Fukuyama tri-protected polyamine intermediate. Arkivoc 2019;2019:168–77. doi:10.24820/ark.5550190.p010.895.

[15] Zamperini C, Maccari G, Deodato D, Pasero C, D'Agostino I, Orofino F, et al. Identification, synthesis and biological activity of alkyl-guanidine oligomers as potent antibacterial agents. Sci Rep 2017;7:8251. doi:10.1038/ s41598-017-08749-6.

[16] Deodato D, Maccari G, De Luca F, Sanfilippo S, Casian A, Martini R, et al. Biological characterization and in vivo assessment of the activity of a new synthetic macrocyclic antifungal compound. J Med Chem 2016;59:3854–66. doi:10.1021/acs.jmedchem.6b00018.
[17] Prasad R, Balzi E, Banerjee A, Khandelwal NK. All about CDR transporters: Past, present, and future. Yeast 2019;36:223–33. doi:10.1002/yea.3356.
[18] Khandelwal NK, Chauhan N, Sarkar P, Esquivel BD, Coccetti P, Singh A, et al. Azole resistance in a Candida albicans mutant lacking the ABC transporter CDR6/ROA1 depends on TOR signaling. J Biol Chem 2018;293(2):412–32. doi:10.1074/jbc.M117.807032.
[19] Jiang L, Xu D, Chen Z, Cao Y, Gao P, Jiang Y. The putative ABC transporter encoded by the orf19.4531 plays a role in the sensitivity of Candida albicans cells to azole antifungal drugs. FEMS Yeast Res 2016;16(3) pii:fow024–8. doi:10.1093/femsyr/fow024.
[20] Reference Method for Broth Dilution Antifungal Susceptibility Testing of Yeasts; Approved Standard - Third Edition M27-A3. CLSI, Wayne, PA, USA, 2008.
[21] Gietz RD, Schiestl RH, Willems AR, Woods RA. Studies on the transformation of intact yeast cells by the LiAc/SS-DNA/PEG procedure. Yeast 1995;11:355–60. doi:10.1002/yea.320110408.
[22] Lamping E, Monk BC, Niimi K, Holmes AR, Tsao S, Tanabe K, et al. Characterization of three classes of membrane proteins involved in fungal azole resistance by functional hyperexpression in Saccharomyces cerevisiae. Eukaryotic Cell 2007;6:1150–65. doi:10.1128/EC.00091-07.
[23] Huang JX, Cooper MA, Baker MA, Azad MAK, Nation RL, Li J, et al. Drug-binding energetics of human α-1-acid glycoprotein assessed by isothermal titration calorimetry and molecular docking simulations. J Mol Recognit 2012;25:642– 56. doi:10.1002/jmr.2221.
[24] Ha CE, Petersen CE, Park DS, Harohalli K, Bhagavan NV. Investigations of the effects of ethanol on warfarin binding to human serum albumin. J Biomed Sci 2000;7:114–21. doi:10.1159/000025436.
[25] Pasero C, D'Agostino I, De Luca F, Zamperini C, Deodato D, Truglio GI, et al. Alkyl-guanidine compounds as potent broad-spectrum antibacterial agents: chemical library extension and biological characterization. J Med Chem 2018;61:9162–76. doi:10.1021/acs.jmedchem.8b00619.
[26] Murray M, Zhang WV, Edwards RJ. Variation in the response of clozapine biotransformation pathways in human hepatic microsomes to CYP1A2- and CYP3A4-selective inhibitors. Basic Clin Pharmacol Toxicol 2018;122:388–95. doi:10.1111/bcpt.12933.
[27] Patki KC, Moltke Von LL, Greenblatt DJ. In vitro metabolism of midazolam, triazolam, nifedipine, and testosterone by human liver microsomes and recombinant cytochromes p450: role of cyp3a4 and cyp3a5. Drug Metab Dispos 2003;31:938–44. doi:10.1124/dmd.31.7.938.
[28] Galetin A, Ito K, Hallifax D, Houston JB. CYP3A4 substrate selection and substitution in the prediction of potential drug-drug interactions. J Pharmacol Exp Ther 2005;314:180–90. doi:10.1124/jpet.104.082826.
[29] Usmani KA, Tang J. Human cytochrome P450: metabolism of testosterone by CYP3A4 and inhibition by ketoconazole. Curr Protoc Toxicol 2004;20 4.13.1– 4.13.9. doi:10.1002/0471140856.tx0413s20.
[30] Choi MH, Skipper PL, Wishnok JS, Tannenbaum SR. Characterization of testosterone 11 beta-hydroxylation catalyzed by human liver microsomal cytochromes P450. Drug Metab Dispos 2005;33:714–18. doi:10.1124/dmd.104. 003327
[31] Zamperini C, Dreassi E, Vignaroli G, Radi M, Dragoni S, Schenone S, et al. CYPdependent metabolism of antitumor pyrazolo[3,4-d]pyrimidine derivatives is characterized by an oxidative dechlorination reaction. Drug Metab Pharmacokinet 2014;29:433–40. doi:10.2133/dmpk.DMPK-13-RG-094.
[32] Patki KC, Moltke Von LL, Greenblatt DJ. In vitro metabolism of midazolam, triazolam, nifedipine, and testosterone by human liver microsomes and recombinant cytochromes p450: role of cyp3a4 and cyp3a5. Drug Metab Dispos 2003;31:938–44. doi:10.1124/dmd.31.7.938.
[33] Chowdhary A, Sharma C, Meis JF. Candida auris: A rapidly emerging cause of hospital-acquired multidrug-resistant fungal infections globally. PLoS Pathog 2017;13:e1006290 –10. doi:10.1371/journal.ppat.1006290.

[34] Jiang L, Xu D, Chen Z, Cao Y, Gao P, Jiang Y. The putative ABC transporter encoded by the orf19.4531 plays a role in the sensitivity of Candida albicans cells to azole antifungal drugs. FEMS Yeast Research 2016;16 fow024–8. doi:10.1093/femsyr/fow024.
[35] Decottignies A, Grant AM, Nichols JW, de Wet H, McIntosh DB, Goffeau A. ATPase and multidrug transport activities of the overexpressed yeast ABC protein Yor1p. J Biol Chem 1998;273:12612–22.
[36] Liu TT, Znaidi S, Barker KS, Xu L, Homayouni R, Saidane S, et al. Genome-wide expression and location analyses of the Candida albicans Tac1p regulon. Eukaryotic Cell 2007;6:2122–38. doi:10.1128/EC.00327-07.
[37] Huang JX, Cooper MA, Baker MA, Azad MAK, Nation RL, Li J, et al. Drug-binding energetics of human α-1-acid glycoprotein assessed by isothermal titration calorimetry and molecular docking simulations. J Mol Recognit 2012;25:642– 56. doi:10.1002/jmr.2221.
[38] Nelson DR. Cytochrome P450 Nomenclature, 2004. Cytochrome P450 Protocols, 320. New Jersey: Humana Press, Totowa, NJ; 2006. p. 1–10. doi:10.1385/ 1-59259-998-2:1.
[39] Rendic S, Carlo FJD. Human cytochrome P450 enzymes: a status report summarizing their reactions, substrates, inducers, and inhibitors. Drug Metab Rev 2010;29:413–580. doi:10.3109/03602539709037591.
[40] Zhang Y, Huo M, Zhou J, Xie S. PKSolver: An add-in program for pharmacokinetic and pharmacodynamic data analysis in Microsoft Excel. Comput Methods Programs Biomed 2010;99:306–14. doi:10.1016/j

FIGURE CAPTIONS

Fig. 1. Chemical structure of BM1.

Fig. 2. Susceptibility test of the S. cerevisiae mutant strains AD-CDR6 and AD(1- 8)u− to BM1 and, as reference, to BER (Berberine) and R123 (Rhodanine 123). A 5- fold serial dilution of each strain was spotted on to YEPD (Ctr) and YEPD with BER (75 μg/mL), BM1 (4.65 μg/mL), and R123 (4 μg/mL) agar plates and grown for 48 h at 30 °C.

Fig. 3. CDR6 expression study in clinical isolates of C. albicans and its impact on susceptibility to BM1. (a) Semiquantitative RT-PCR of CDR6 in Gu4 vs Gu5 clinical isolates of C. albicans. (b) C. albicans clinical isolates growth comparison by spot dilution assay in presence of FLC (fluconazole, 16 μg/mL) and BM1 (4.65 μg/mL).

Fig. 4. Inhibition of CYP3A4 isoform activity by BM1 (panel A) and ketoconazole (panel B), measured as concentration of β6-hydroxytestosterone (β6-OH-TST), compared to the control (Ctrl) mix in absence of compounds. Statistical significance for BM1 has been evaluated through Graphpad InStat v. 3.02 using Student's t-test.

Fig. 5. Plasmatic levels of BM1 at two different doses after intravenous administration. The smaller chart is in semi-log scale.

Fig. 6. Quantity levels of BM1 found in different organs after 24 h intravenous inoculum at two different dose regimens (2 and 10 mg/kg body weight) expressed in μg/g of tissue.

Fig. 7. Analysis of BM1 level in rats. On the left, kidney, bladder, liver, and brain levels after 6 days (2 mg/kg dosage) expressed as μg/g of tissue. On the right, levels of BM1 in urine after 24, 48, 72 and 144 h (μg/mL of urines).

Table 1. Antifungal activities of compound BM1 against various Candida species. MICs and MBCs are reported in µg/mL as a range (lowest and highest observed MIC for each species). The number of tested strains per species is reported in parenthesis.

MIC and MBC range (µg/mL) against Candida species											
C. albicans (10)		C. tropicalis (10)		C. parapsilosis (10)		C. glabrata (10)		C. krusei (10)		C. auris (18)	
MIC	MBC	MIC	MBC	MIC	MBC	MIC	MBC	MIC	MBC	MIC	MBC
0.125-2	2 2-4	2	2-4	8-16	32-64	32-64	64-128	8-64	64-128	8-64	128-256

MBC, minimum bactericidal concentration; MIC, minimum inhibitory concentration

Table 2. In vitro water solubility, passive permeability and binding with human serum proteins of compound BM1.

LogS[a] (log mol/L)	**Membrane permeation**[b] Papp[c] x 10^{-6} (cm/s)	**Metabolic Stability**[d] (%)	**Major Metabolitese**[d] (%)	**Binding human serum proteins** K_d (µM)	
				AGP	**HSA**
2.61	< 0.1	95	M+OH (5)	12.2	212.1

a Aqueous solubility was determined by means of LC-MS method 1 reported in supporting data (log mol/L). b Membrane permeation was determined with a PAMPA technique. c Apparent Permeability. d The human liver microsome stability is expressed as percentage of unmodified parent drug. e M = mass of the parent drug; the percentage of metabolite experimentally determined via LC-MS is reported in parentheses. e Dissociation constant (Kd) values are measured by means of indirect fluorescence method.

Table 3. PK parameters for compound BM1.

PK Parameter	**Unit**	**10 mg/kg IV Value**	**2 mg/kg IV Value**	**20 mg/kg PO Value**
t1/2	h	13.01	15.68	n.d.
Tmax	h	0.08	0.08	n.d.
Cmax	µg/mL	2.78	0.87	n.d.
C_0	µg/mL	3.15	1.14	n.d.
$AUC_{0\rightarrow 24h}$	µg/mL*h	6.11	1.11	n.d.
$AUC_{0\rightarrow \infty}$	µg/mL*h	1.44	7.83	n.d.
$AUMC_{0\rightarrow \infty}$	µg/mL*h^2	108.27	20.82	n.d.
MRT0→∞	H			n.d.
Vz	(mg/kg)/(µg/mL)	23.95	31.40	n.d.
Cl	(mg/kg)/(µg/mL)/h	1.28	1.39	n.d.

Data calculated with PKSolver. [40] Cmax: maximum concentration observed. C0: concentration at time 0 (estimated). Tmax: time of maximum concentration observed. MRT: mean residence time. AUC: area under the curve. AUMC: area under the first moment curve. Vz: volume of distribution. Cl: clearance. t1/2: halflife. n.d.: not detected. IV: intravenous. PO: per os.

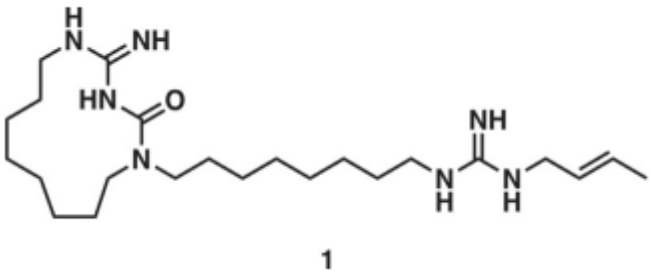

FIGURE 1

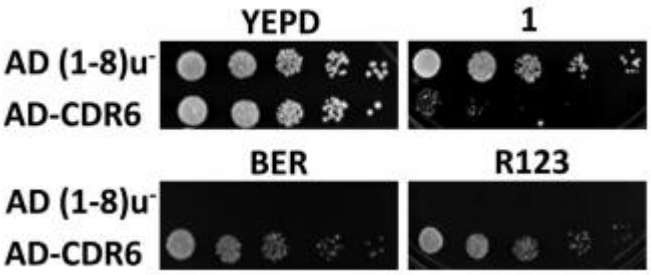

FIGURE 2

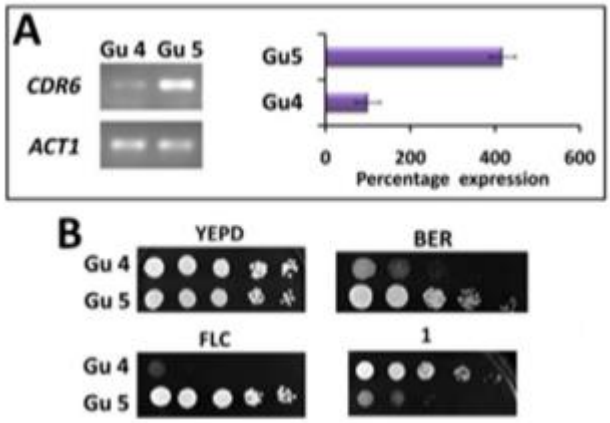

FIGURE 3

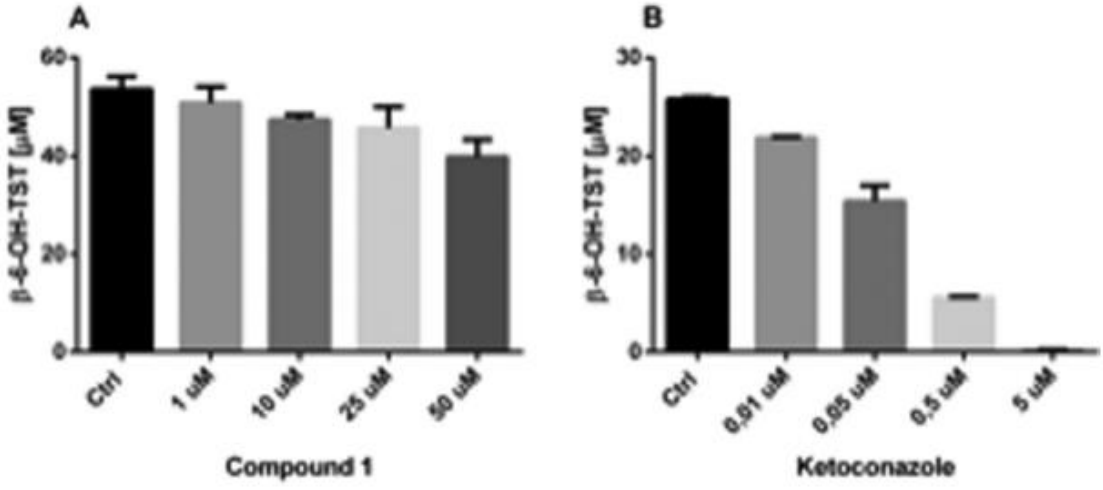

FIGURE 4

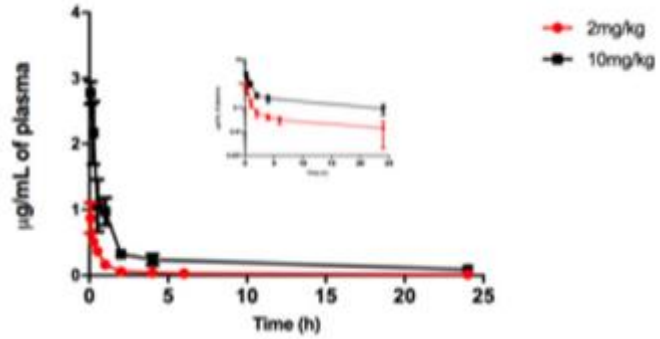

FIGURE 5

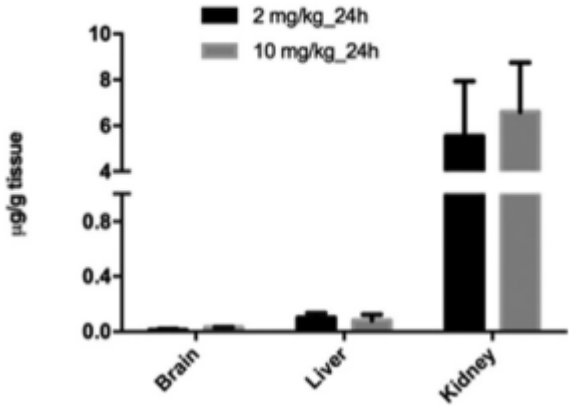

FIGURE 6

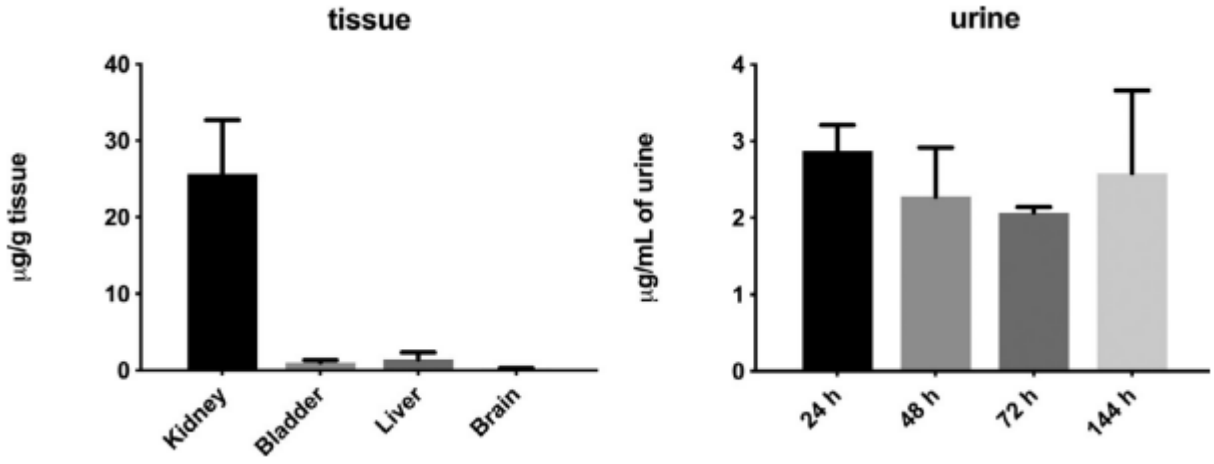

FIGURE 7